Computer Aided Surgery, September 2006; 11(5): 231–239

informa
healthcare

BIOMEDICAL PAPER

Visualization and navigation system development and application for stereotactic deep-brain neurosurgeries

TING GUO[1], KIRK W. FINNIS[3], ANDREW G. PARRENT[2], & TERRY M. PETERS[1]

[1]*Robarts Research Institute and Biomedical Engineering Graduate Program, University of Western Ontario, London, Ontario;* [2]*Department of Neurosurgery, The London Health Sciences Centre, London, Ontario; and* [3]*Atamai Inc., London, Ontario, Canada*

(Received 28 February 2006; accepted 23 June 2006)

Abstract

We present the development of a visualization and navigation system and its application in pre-operative planning and intra-operative guidance of stereotactic deep-brain neurosurgical procedures for the treatment of Parkinson's disease, chronic pain, and essential tremor. This system incorporates a variety of standardized functional and anatomical information, and is capable of non-rigid registration, interactive manipulation, and processing of clinical image data. The integration of a digitized and segmented brain atlas, an electrophysiological database, and collections of final surgical targets from previous patients facilitates the delineation of surgical targets and surrounding structures, as well as functional borders. We conducted studies to compare the surgical target locations identified by an experienced stereotactic neurosurgeon using multiple electrophysiological exploratory trajectories with those located by a non-expert using this system on 70 thalamotomy, pallidotomy, thalamic deep-brain stimulation (DBS), and subthalamic nucleus (STN) DBS procedures. The average displacement between the surgical target locations in both groups was 1.95 ± 0.86 mm, 1.83 ± 1.07 mm, 1.88 ± 0.89 mm and 1.61 ± 0.67 mm for each category of surgeries, respectively, indicating the potential value of our system in stereotactic deep-brain neurosurgical procedures, and demonstrating its capability for accurate surgical target initiation.

Keywords: *Deep-brain stimulation, thalamotomy, pallidotomy, navigation, neurosurgery*

Introduction

The three major surgical options available for the treatment of Parkinson's disease and essential tremor are the creation of a small lesion, placement of deep-brain stimulators, and implantation of stem cells [1–3]. The motor nuclei of the thalamus, the internal segment of the globus pallidus (GPi), and the subthalamic nucleus (STN) are the three surgical targets for the first two commonly adopted procedures. The entire surgical procedure primarily comprises pre-operative surgical target/trajectory planning, intra-operative electrophysiological exploration and confirmation, and the final lesion creation or stimulator placement. To achieve the best surgical outcome with minimal invasiveness, the surgeon must accurately localize the surgical target during the first two steps. The first phase is carried out based on pre-operative MR or CT images with the assistance of printed [4–6] or digital [7–10] anatomical atlases. In addition to the anatomical information derived from the medical images and brain atlases, functional information, obtained from invasive intra-operative

Correspondence: Ting Guo / Terry M. Peters, Imaging Research Laboratories, Robarts Research Institute, P.O. Box 5015, 100 Perth Drive, London, Ontario, Canada N6A 5K8. Tel: (519) 663-5777 ext. 34136 (T.G.) or ext. 34159 (T.M.P.). Fax: (519) 663-3900. Email: tguo@imaging.robarts.ca / tpeters@imaging.robarts.ca

Part of this research was previously presented at the 8th International Conference on Medical Image Computing and Computer-Assisted Intervention (MICCAI 2005) in Palm Springs, CA, October 2005.

ISSN 1092-9088 print/ISSN 1097-0150 online ©2006 Informa UK Ltd
DOI: 10.1080/10929080600997232

electrophysiological measurements in the second step, is also required to refine the optimal surgical targets, to characterize tissue function, and to map somatotopy.

A number of printed atlases, e.g., those of Schaltenbrand and Wahren [4], Talairach and Tournoux [5], and Van Buren and Borke [6], have been produced. However the effectiveness of printed atlases is significantly limited by their inherent disadvantages, such as the fixed 2D representation, the fact that individual brains may show considerable variations in anatomical structure as compared to the atlas, and the unsuitability of the atlas images for digital processing. To overcome these problems, several groups have implemented computerized versions of some of these atlases [7–10]. Once integrated into computer surgical planning and guidance systems, the digitized atlases can be rigidly [11,12] or non-rigidly [10,13,14] aligned and fused with individual pre-operative brain images to facilitate the identification of surgical targets. Nevertheless, existing anatomical atlases should be employed cautiously for planning stereotactic procedures because of their inherent limitations. Therefore, target locations estimated with digitized anatomical atlases scaled to individual patient brain images can only be used as initial approximations of the true locations of the targets. To overcome the lack of deep-brain anatomical information provided by standard T1-weighted pre-operative MR images, where the targets for the surgical treatment of Parkinson's disease cannot be distinguished from their surrounding structures, some investigators have employed T2-weighted MRI to better visualize these targets, especially the STN [15–18]. Although this approach has shown promise, the correspondence between the targets defined on these images and those refined with electrophysiological explorations is not consistent [19,20]. Currently, these electrophysiological measurements, including microelectrode recording (MER) and electrical stimulation data, are acquired during the surgical procedures with multiple invasive exploratory trajectories, which may damage the brain tissue. To improve pre-operative surgical target planning accuracy, reduce the need for invasive intra-operative exploration, and decrease procedure-related complications, electrophysiological atlases [21–23] and databases [24] containing data from multiple patients have been developed. In general, these atlases and databases have been normalized to a standard brain template to provide additional standardized electrophysiological information prior to surgery. The electrophysiological atlas proposed by D'Haese et al. [22] classifies the intra-operative microelectrode recording signals according to their firing rate and parameters measuring phasic activities, and maps the color-coded values of these features to the atlas. These established techniques for electrophysiological mapping provide probabilistic maps of deep-brain electrophysiological activity and are valuable in establishing the relationship between brain functional organization and anatomic structures, and in estimating the surgical targets [21–26].

The work described in this paper extends the work of Finnis et al. [24] relating to the development of probabilistic functional databases through the construction of a comprehensive neurosurgical system and its clinical validation. Here, we present an improved 3D visualization and navigation system for stereotactic functional deep-brain neurosurgery planning and guidance. We conducted studies to evaluate the effectiveness of this system in surgical targeting for thalamotomy, pallidotomy, thalamic deep-brain stimulation (DBS), and STN DBS procedures. By integrating the electrophysiological database, digitized 3D brain atlases [4], segmented deep-brain nuclei, and categorized surgical targets from previous procedures, along with representations of instruments, our system offers several advantages: (1) interactive display of linked patient and standard brain images; (2) 3D representation of the deep-brain nuclei; (3) accurate non-rigid accommodation of anatomical variability; (4) simultaneous and/or independent manipulation of multiple trajectories; (5) hardware and operating system independence; and (6) intuitive graphical user interface. Once non-rigidly mapped to a patient brain space, the standardized functional and anatomical data incorporated in this system play a crucial role in both pre-operative surgical target planning and intra-operative surgical guidance.

This paper is organized as follows. The next section describes the construction of the electrophysiological database and the integration of the neurosurgical system. This is followed by a discussion of the implementation of this system in actual surgical procedures. Finally, we present the outcome of clinical studies, and discuss the significance and possible limitations of our system.

Materials and methods

Construction of the functional database

Subjects. Data from 140 patients (83 male, 57 female, age 21–83 years, mean age 60 years) who had undergone a total of 187 surgeries (54 thalamotomy, 58 pallidotomy, 21 thalamic DBS, 5 pallidus DBS, and 49 STN DBS) for symptomatic treatment of Parkinson's disease, chronic pain, essential tremor, etc., at London Health Sciences Centre (LHSC) were incorporated in the construction of the

functional database. Of these patients, 103 were diagnosed with Parkinson's disease, 22 with essential tremor, 6 with chronic pain, 4 with dystonias, 1 with torticollis, and 4 with tremor. Each specific surgical procedure was determined by a team of specialists consisting of a neurologist, a neurosurgeon, a neurophysiologist and a neuropsychologist.

MRI data. We used a 3D SPGR sequence (TR/TE 8.9/1.9 ms, flip angle 20°, NEX 2, voxel size 1.17 mm × 1.17 mm × 1 mm, dimensions 256 × 256 × 248) to acquire pre-operative T_1-weighted MR images of the patients with a 1.5T GE Signa scanner. T_2-weighted MR images were also obtained with the same scanner using 2D fast spin-echo sequence (TR/TE 2800/110 ms, flip angle 90°, NEX 4, voxel size 1.0 mm × 1.0 mm × 1.5 mm, spacing 0, coronal acquisition dimensions 256 × 256 × 21, axial acquisition dimensions 256 × 256 × 20) for STN DBS procedures. The Leksell G stereotactic frame (Elekta Instruments AB, Stockholm, Sweden) with attached MR-compatible localizer was applied to each patient immediately before imaging.

Intra-operative electrophysiological data. A comprehensive coding scheme was created to organize the intra-operative micro-recording, micro-stimulation and macro-stimulation data. The electrophysiological data of each patient were coded and recorded in the coordinate system of his or her pre-operative MR image space to help the neurosurgeon correlate the anatomical brain structures with functional organization.

Collection of functional data. To generalize the use of electrophysiological data acquired from each individual surgical procedure, we employed a high-performance rapid non-rigid registration approach [27] to transform and normalize the electrophysiological data from each patient brain space to a standard reference brain coordinate system [28] known as the Colin27 brain template. The Colin27 (or CJH-27) brain dataset with high SNR is used extensively by many research groups. It allows definition of fine anatomical details within the deep brain. In the current study, we adopted it as the reference MRI brain template (the registration target). Colin27 was obtained by rigidly registering 26 of the 27 T_1-weighted MR brain images ($20 \times 1\,mm^3$: TR/TE 18/10 ms, flip angle 30°, NEX 1; $7 \times 0.78\,mm^3$: TR/TE 20/12 ms, flip angle 40°, NEX 1) of the same healthy individual to the 27^{th} image and averaging them into the International Consortium for Brain Mapping (ICBM) brain space [29]. To construct our functional database, we first registered the pre-operative brain image of each patient to the Colin27 brain template to establish the 3D transformation described by the deformation grid. We then applied each 3D non-rigid transformation acquired from the previous step to map the functional data from each patient image to the Colin27 brain space. Finally, we collected the non-rigidly registered functional data into our standard databases, categorized according to the characteristics of the surgical procedures. The population-based functional databases can then be applied to an individual patient using the inverse non-rigid transform.

Image registration. As mentioned previously, image registration is necessary to implement our functional database construction, as well as to use the database in surgical planning and guidance procedures. Two registration steps are required. The first frame-to-image registration step generates the rigid-body transformation that maps the coordinates of patient image-space to the stereotactic frame coordinate system. The second data-to-database and database-to-patient registration step establishes the non-rigid 3D transformation matrix and displacement grid, which maps the functional data from each patient brain space to the standard reference template, and vice versa. Our neurosurgical system allows both semi- and fully automatic frame-to-image registrations. By automatically extracting the fiducial lines and points of the MR localizer, our "frame-finder" algorithm can robustly register the image coordinates to the stereotactic frame space at the sub-voxel level for both MR and CT images in approximately 1.5 seconds. A semi-automatic registration is also available to perform the frame-to-image registration in some exceptional cases. To achieve the non-rigid registration, we employed the AtamaiWarp algorithm [27], a completely unsupervised intensity-based multi-resolution registration approach, built using standard VTK classes, to accommodate the inter-subject anatomical variability between each patient brain image and the Colin27 reference brain space. AtamaiWarp optimizes the registration in the deep-brain region enclosed within a user-defined volume mask and requires 8–12 min on a dual PIII 933MHz machine to perform the deformation with an average registration error of 1.04 mm ± 0.65mm [30]. The algorithm also generates a global affine transformation between the two images, as well as a deformation grid.

Integration of the neurosurgical visualization and navigation system

Our comprehensive surgical visualization and navigation system is integrated with the following

standardized and normalized functional and anatomical information.

Electrophysiological database. We expanded the previous version of the electrophysiological database developed by Finnis et al. [24], containing data from 106 procedures performed on 88 patients, to the current version comprised of data from 187 procedures on 140 patients. The intra-operatively obtained electrophysiological data, coded with respect to particular firing patterns, specific body reactions, and certain anatomical regions, can be retrieved from the database and displayed in two different forms: clusters of spheres in 3D space or density maps on three intersecting orthogonal 2D image planes. Properties of the selected functional data, e.g., color, opacity and shading, can be adjusted to facilitate interpretation of the search results.

Digitized brain atlas and segmented deep-brain nuclei. Because of its extensive use in the neuroscience community, the well-established stereotactic brain atlas of Schaltenbrand and Wahren [4] was non-rigidly mapped to the Colin27 brain space to serve as one of our anatomical references. Different brain structures can be easily distinguished according to the different colors assigned to them. We also segmented each deep-brain nucleus based on its anatomical representation in this atlas. The segmented deep-brain nuclei can be displayed as either 3D objects or as triangulated meshes allowing visualization of trajectories inside each nucleus. This permits the probe trajectories to be placed at optimal functional subdivisions of certain nuclei, such as the dorsolateral STN [31], the posterolateral part of the GPi [32], and the Vim of the thalamus [33]. The centroid of each segmented deep-brain nucleus can be calculated automatically and represented as a sphere.

Final surgical target collections. During each surgical procedure, the locations of the final targets in patient brain space were saved and non-rigidly registered to Colin27. The registered final surgical target locations were collected into one of eight groups categorized by the characteristic of the surgery. These groups contain data from 37 left and 17 right thalamotomies, 30 left and 28 right pallidotomies, 11 left and 10 right thalamic DBS procedures, and 27 left and 22 right STN DBS procedures. We can non-rigidly map the center of mass (COM) and the statistical map of a cluster of final surgical targets to the pre-operative MR image of each individual patient for surgical target initialization.

Surgical instrument representation. Up to five multiple virtual probes, mimicking their physical counterparts, can be manipulated simultaneously or independently to simulate the real surgical procedures. The inter-probe distance is modifiable according to requirements. When implemented with the "frame-finder" algorithm, this system also provides simultaneous display of the tip positions for these trajectories in both image space and stereotactic frame space.

Visualization and navigation platform. The primary graphic user interface of our system consists of two major components: the image display area and the function control panel (Figure 1). The 3D image volume and three orthogonal 2D slices of a patient and those of the standard brain template can be interactively displayed in the adjustable viewing windows of the display area. The system is capable of registering and fusing the digitized brain atlases and T2-weighted images with the pre-operative patient and standard images. The opacity and window/level of each of these images can be modified independently for the best visual effect. Three-dimensional images may be reformatted along arbitrary axes. The functional information, along with the anatomical references provided by the digitized atlases and segmented nuclei, greatly facilitates planning of surgical targets (Figure 2). Within this environment, coded functional data, plotted directly onto each patient's pre-operative image along a virtual trajectory that corresponds to the position and orientation of the physical probe, can be non-rigidly registered to the standard brain template automatically. The intra-operatively acquired data are saved in a text file whose header contains the code describing the patient information and specifications of the probes used during the procedure. Meanwhile, these data after mapping to Colin27 are stored in the functional database.

Clinical application

Standard surgical planning procedure

Each patient recruited to this study had his or her procedure planned by the neurosurgeon (A.G.P.) using the standard planning technique immediately after pre-operative MRI acquisition. The benchmark anatomical structures such as the anterior commissure (AC) and posterior commissure (PC) in the MR image were first identified, then the image was reconstructed to align with the AC-PC orientation. The initial target point for the procedure was determined based on its location relative to AC and PC (pallidotomy: 2–4 mm anterior to the mid AC-PC point, 19–22 mm lateral to the midline line, and 4–6 mm below the AC-PC plane; thalamotomy/thalamic

DBS: 4–8 mm anterior to the PC, 12–15 mm lateral to the midline, and 0–2 mm superior to the AC-PC plane; STN DBS: 3 mm posterior to the mid AC-PC point, 11–12 mm lateral to the midline, and 4–6 mm below the AC-PC plane), and linear Talairach mapping of the nearest atlas section from the Schaltenbrand and Wahren atlas [4]. The final surgical target was refined through multiple electrophysiological recording and stimulus/response measurements to optimally ameliorate the symptoms.

System-based planning procedure

Independently of the neurosurgeon, a non-expert (T.G.) familiar with deep-brain anatomy estimated the surgical target location and trajectory orientation for the creation of a lesion or placement of a DBS electrode, using the neurosurgical visualization and navigation system integrated with the customized functional and anatomical references. For each case, the pre-operative MR image of each patient was loaded into our system and non-rigidly registered to the standard Colin27 brain template. The 3D transformation and non-rigid displacement grid file generated by registration were then applied to map the data in the electrophysiological database, the collection of previous surgical targets, and the digitized Schaltenbrand atlas, as well as segmented deep-brain nuclei, to the patient brain image. We conducted three retrospective studies and one prospective study to evaluate the effectiveness of this neurosurgical visualization and navigation system for surgical targeting by comparing the target locations estimated by the non-expert with those identified by the neurosurgeon. We employed 20 thalamotomies (10 left, 10 right), 20 pallidotomies (10 left, 10 right), and 10 thalamic DBS procedures (5 left, 5 right) for the retrospective studies, and 20 STN DBS procedures (10 left, 10 right) for the prospective study.

Results

Assessment of the non-rigid registration algorithm

Various non-rigid image registration algorithms for the mapping of digitized brain atlases and electrophysiological databases have been published and widely used in medical imaging research. However, assessing these algorithms remains difficult due to the lack of "gold standards." Since accurate registration plays a critical role in localizing surgical targets with reference to standardized anatomical and functional information, it is necessary to determine how much the registration algorithm used in our studies [27] affects the clinical results. As described earlier, we have eight databases for the collection of previous patient surgical targets. Registering the collection of previous final surgical targets from the standard database to an individual patient image yields a probabilistic estimation of the target location for the patient. To assess our registration algorithm clinically, a cluster of 26 left STN DBS surgical targets contained in the database was non-rigidly registered to the images of 10 patients who had undergone similar surgical procedures. Data from 21 right STN DBS targets were mapped to the images of 10 patients undergoing right STN DBS. Similarly, 36 left and 16 right thalamotomy, 29 left and 27 right pallidotomy, and 10 left and 9 right thalamic DBS surgical targets were also transformed to the images of 10, 10, 10, 10, 5 and 5 patients who had undergone these same surgeries, respectively. Table I shows the comparison between the center of mass (or the most significant position on the probability map) of database-initialized locations and the actual surgical targets for the 70 procedures. The results demonstrate that the registration algorithm performs well within homogeneous regions in the deep brain. Although the maximum average distance between the registered centroid of the collection of surgical targets in the databases and the actual target locations is 2.33 ± 0.80 mm, this technique nevertheless provides a suitable initial estimate of the pre-operative surgical target, which may be further refined with additional functional and anatomical information available on the neurosurgical system.

Application of the segmented deep-brain nuclei

We have previously demonstrated that the Atamai-Warp algorithm performs well in non-rigid

Table I. Absolute differences between database-initialized and real surgical targets.

	Pallidotomy				Thalamotomy				Thalamic DBS				STN DBS			
Difference	x	y	z	dis	x	y	z	dis	x	y	z	dis	x	y	z	dis
Mean (mm)	1.31	1.10	1.42	2.33	1.37	1.09	1.44	2.18	1.19	1.30	1.35	2.29	1.25	1.27	1.14	2.21
Max (mm)	2.33	2.41	2.75	3.96	2.17	2.77	2.52	3.65	2.20	2.48	2.14	3.55	2.19	2.68	2.38	3.72
Min (mm)	0.57	0.77	0.61	1.52	0.65	0.48	0.75	1.21	0.41	0.52	0.50	1.26	0.63	0.79	0.33	1.48
Std (mm)	0.62	0.68	0.67	0.80	0.51	0.78	0.69	0.77	0.60	0.71	0.68	0.71	0.53	0.61	0.74	0.73

registration of inter-subject brain images [30], and therefore the atlas-based segmented deep-brain nuclei transformed to a patient brain space using this technique should demonstrate a high percentage of overlap with the patient's own nuclei. The anatomical information provided by a specific segmented nucleus registered to a patient with Atamai-Warp (Figure 3) should be capable of indicating the relative spatial location of the optimal surgical target within the nucleus after transformation. At our institution, the region of the Vim close to the border with the sensory thalamus (Vc) is considered to be the optimal target for tremor arrest with thalamotomy or thalamic DBS, the posterolateral part of the GPi has been adopted as the ideal destination for pallidotomy, while the dorsolateral portion of STN is regarded as the most effective stimulation site in STN DBS. We compared the Euclidean distance between the centroid of the registered segmented Vim, GPi or STN and the real target location of each patient who had been subject to a thalamotomy, pallidotomy or STN DBS procedure, respectively (Table II). In our study, more than 72% of the actual surgical targets were located at the expected positions relative to the corresponding centroids.

Detection of the effectiveness in surgical targeting

Clinical data from the thalamotomy, pallidotomy, thalamic DBS and STN DBS procedures were included in our studies. We evaluated the effectiveness of our system in surgical targeting on 20 thalamotomies, 20 pallidotomies and 10 thalamic DBS procedures retrospectively, and on 20 STN DBS procedures prospectively (Table 3). The average distance

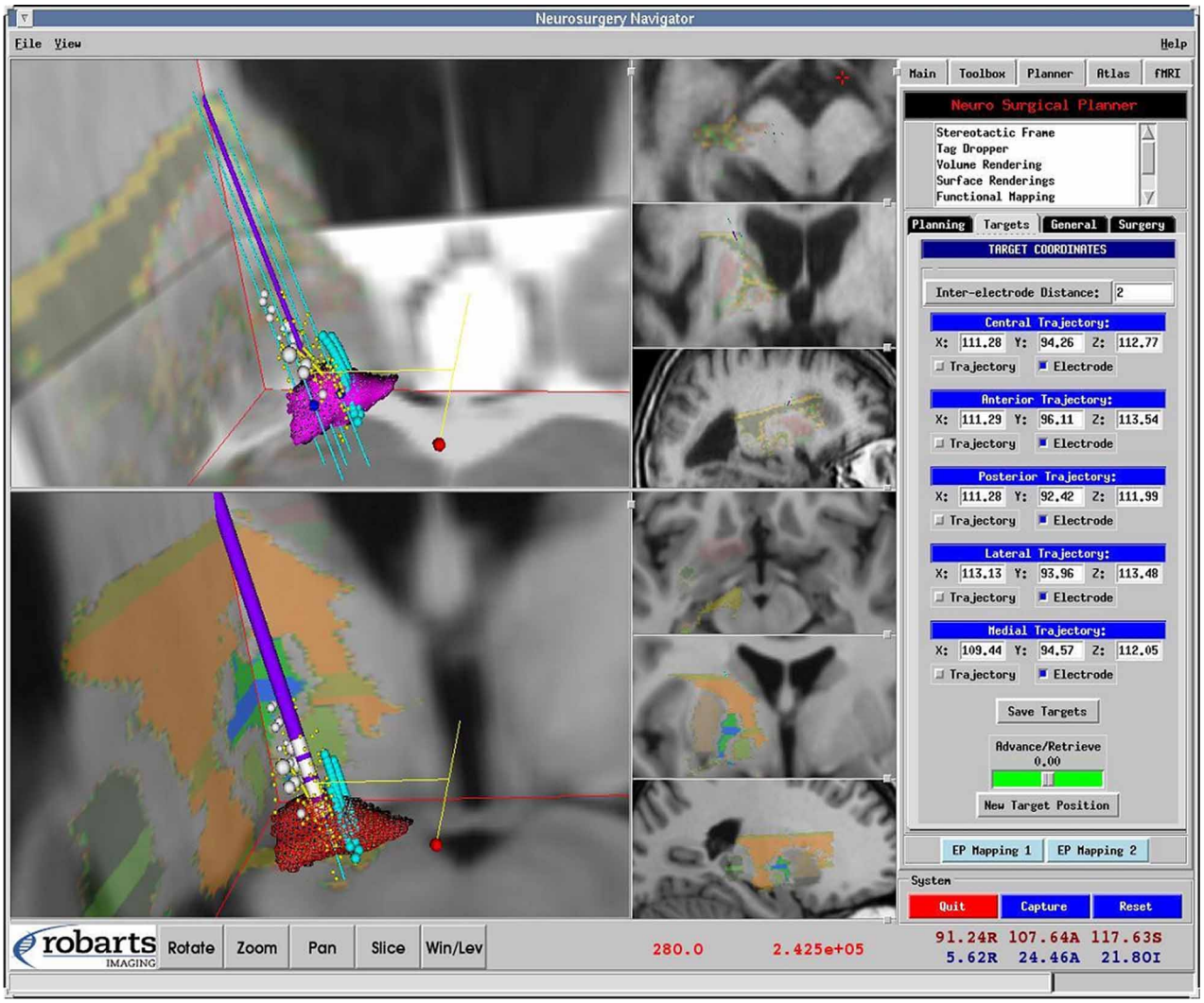

Figure 1. The primary graphical user interface of the system displays the 3D image volume and 2D slices of a patient (top) and those of the standard brain template (bottom). The digitized atlas is registered and fused with each image. A T2-weighted image fused with the patient image is also shown. The control panel shows the tip locations for the five probes. [Color version available online.]

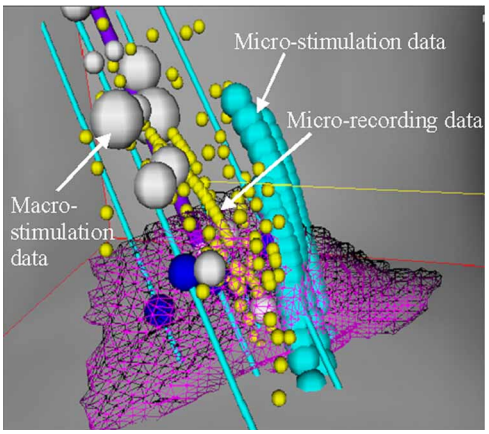

Figure 2. The magnified version of Figure 1. The purple line in the center represents the central electrodes. The cyan lines parallel to the central line represent surgical trajectories. The small yellow spheres represent micro-recording data, the larger cyan spheres micro-stimulation data, and the still larger white spheres macro-stimulation data. The mesh object is the sub-thalamic nucleus (STN); the segmented STN and electrophysiological data are non-rigidly registered from the standard brain space to the patient brain image. [Color version available online.]

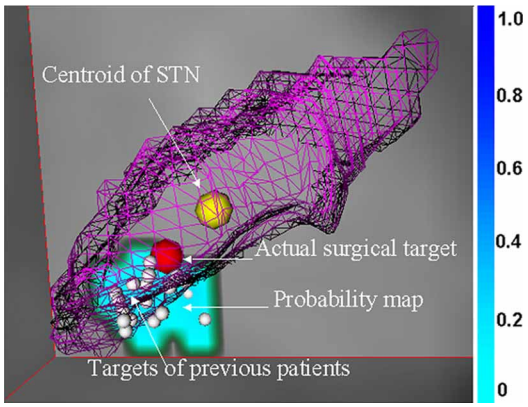

Figure 3. Segmented sub-thalamic nucleus (STN) registered with AtamaiWarp. The mesh object is the STN. The yellow sphere is the centroid of the STN, the red sphere is the actual surgical target, and the white spheres represent surgical targets of previous patients. The color-coded map is the probability map of a collection of left STN DBS targets. [Color version available online.]

between the non-expert-planned surgical targets and the expert-localized ones was 1.95 ± 0.86 mm for thalamotomies, 1.83 ± 1.07 mm for pallidotomies, 1.88 ± 0.89 mm for thalamic DBS procedures, and 1.61 ± 0.67 mm for STN DBS procedures. In addition, the surgical sites determined using the combined information from both the electrophysiological database and the anatomical resources were closer to the final surgical targets chosen by the neurosurgeon than those defined either by standard image-based techniques or by the mapping of a cluster of surgical targets onto the pre-operative images. These residuals indicate that an initial estimation of target location, made on the basis of this software, is typically within 2 mm of the real surgical target. Therefore, the final surgical target can be reached by slightly refining the initiation of the target position estimated using this system with greatly reduced electrophysiological exploration. In this way, the duration of pre-operative target/trajectory planning and intra-operative electrophysiological exploration can be significantly shortened without compromising surgical accuracy and precision.

Discussion

We have described the development and application of a visualization and navigation system for stereotactic deep-brain neurosurgery. Studies conducted to evaluate the performance of this system in real

Table II. Absolute differences between centroids of segmented nuclei after non-rigid registration and real surgical targets.

	Pallidotomy				Thalamotomy/thalamic DBS				STN DBS			
Difference	x	y	z	dis	x	y	z	dis	x	y	z	dis
Mean (mm)	1.55	1.60	1.18	2.53	1.16	1.13	1.35	2.24	1.36	1.88	0.85	2.80
Max (mm)	2.43	2.45	1.76	3.17	1.99	2.38	1.86	3.09	2.32	3.23	1.45	3.57
Min (mm)	0.22	0.51	0.30	0.97	0.18	0.36	0.40	1.05	0.31	0.01	0.23	1.21
Std (mm)	0.61	0.93	0.77	0.83	0.69	0.97	0.72	0.79	0.74	1.15	0.60	0.87

Table III. Absolute differences between non-expert-estimated and real surgical targets.

	Pallidotomy				Thalamotomy				Thalamic DBS				STN DBS			
Difference	x	y	z	dis	x	y	z	dis	x	y	z	dis	x	y	z	dis
Mean (mm)	0.61	0.65	0.87	1.83	0.48	0.73	0.75	1.95	0.43	0.70	0.74	1.88	0.55	0.68	0.70	1.61
Max (mm)	1.42	1.33	1.34	2.79	1.29	1.30	1.51	2.69	1.22	1.26	1.38	2.41	1.31	1.43	1.39	2.82
Min (mm)	0.10	0.27	0.33	0.58	0.23	0.28	0.35	0.62	0.17	0.12	0.35	0.54	0.06	0.30	0.2	0.65
Std (mm)	0.49	0.39	0.31	1.07	0.51	0.38	0.40	0.86	0.48	0.40	0.32	0.89	0.50	0.38	0.35	0.67

clinical situations demonstrated its beneficial role in simplifying pre-operative planning procedures and in accurately localizing surgical targets. The great potential of this visualization and navigation system was indicated by the results of the retrospective and prospective studies. When employed both pre- and intra-operatively for planning surgical trajectories, and for plotting and analyzing functional data in the patient's pre-operative image space during each case of the prospective study, our system demonstrated its efficacy in assisting the identification of surgical loci for STN DBS procedures. Although the studies for thalamotomy, pallidotomy, and thalamic DBS surgical planning and guidance were carried out retrospectively, the surgical target estimation process for each case was performed in the same manner as for the STN DBS procedures. The visualization capabilities, designed for presentation of all relevant functional and anatomical data along with multiple virtual surgical instruments, have made it possible to simulate actual surgical procedures. Using the automatically calculated frame-to-MRI transforms, the intra-operatively acquired data can be saved along with the physical information of the patient and specifications of the probes used during the procedure. Once the 3D non-rigid transformation, obtained by registering each patient image to the Colin27 brain template, is applied, these data can be mapped to the standard brain space and stored in the functional database. This work yielded promising results for the application of our system to deep-brain neurosurgical procedures, even without correction for possible brain movement or shift due to leakage of cerebrospinal fluid (CSF) and change in the patient's position.

While only a single neurosurgeon has been involved in this work to date, it is hoped to perform a multi-center study in the future. Despite the difficulty and complexity of accurately segmenting Vim, GPi, and STN on patient image files, comparing the overlapping ratio between the registered segmented deep-brain nuclei of each patient and that of the standard brain atlas could also provide valuable measurements for validation of the registration algorithm. High-quality anatomical and/or histological atlases containing more detailed deep brain information may enhance the accuracy of our system in surgical planning and targeting, and improve the reliability of the correlation between the anatomical structures and the electrophysiological organization. Although this system has reached a stage where prediction of surgical targets/trajectories is encouraging, further clinical evaluation of the long-term surgical outcome is required for thorough validation and application in stereotactic deep-brain neurosurgical procedures.

Acknowledgments

The authors wish to thank Dr. Mark Wachowiak for his help with the paper revision. The authors acknowledge financial support from the Canadian Institutes of Health Research (CIHR), the Ontario Research and Development Challenge Fund (ORDCF), the Canada Foundation for Innovation (CFI), and the Ontario Innovation Trust (OIT).

References

1. Perrier AL, Tabar V, Barberi T, Rubio ME, Bruses J, Topf N, Harrison NL, Studer L. Derivation of midbrain dopamine neurons from human embryonic stem cells. Proc Natl Acad Sci USA 2004;101(34):12543–12548.
2. Andersson E, Tryggvason U, Deng Q, Friling S, Alekssenko Z, Robert B, Perlmann T, Ericson J. Identification of intrinsic determinants of midbrain dopamine neurons. Cell 2006;124(2):393–405.
3. Correia AS, Anisimov SV, Li JY, Brundin P. Stem cell-based therapy for Parkinson's disease. Ann Medicine 2005;37(7):487–498.
4. Schaltenbrand G, Wahren W. Atlas for Stereotaxy of the Human Brain. Stuttgart, Germany: Thieme; 1977.
5. Talairach J, Tournoux P. Co-Planar Stereotaxic Atlas of the Human Brain. Stuttgart, Germany: Thieme; 1988.
6. Van Buren JM, Borke RC. Variations and Connections of the Human Thalamus. Berlin, Germany: Springer; 1972.
7. Nowinski WL, Yeo TT, Yang GL, Dow DE. Atlas-based system for functional neurosurgery. In: Kim YM, editor. Proceedings of SPIE Medical Imaging 1997, Newport Beach, February 1997. SPIE Vol 3031. pp 92–103.
8. Schiemann T, Hoehne KH, Koch C, Pommert A, Riemer M, Schubert R, Thiede U. Interpretation of tomographic images using automatic atlas lookup. In: Robb RA, editor. Proceedings of SPIE Visualization in Biomedical Computing 1994, Rochester, MN, October 1994. SPIE Vol 2359. pp 457–465.
9. Ganser KA, Dickhaus H, Metzner R, Wirtz CR. A deformable digital brain atlas system according to Talairach and Tournoux. Med Image Anal 2004;8(1):3–22.
10. Bertrand G, Olivier A, Thompson CJ. The computerized brain atlas: Its use in stereotaxic surgery. Trans Am Neurol Assoc 1973;98:233–237.
11. Kall BA, Kelly PJ, Goerss S, Frieder G. Methodology and clinical experience with computed tomography and a computer-resident stereotactic atlas. Neurosurgery 1985;17(3):400–407.
12. Lehman RM, Zheng J, Hamilton JL, Micheli-Tzanako E. Comparison of 3-D stereoscopic MR imaging with pre and post lesion recording in pallidotomy. Acta Neurochir (Wien) 2000;142(3):319–328.
13. Collins DL, Holmes CJ, Peters TM, Evans AC. Automatic 3-D model-based neuroanatomical segmentation. Human Brain Mapping 1995;3(3):190–208.
14. St-Jean P, Sadikot AF, Collins DL, Clonda D, Kasrai R, Evans AC, Peters TM. Automated atlas integration and interactive 3-dimensional visualization tools for planning and guidance in functional neurosurgery. IEEE Trans Med Imag 1998;17:672–680.
15. Starr PA, Vitek JL, DeLong M, Bakay RAE. Magnetic resonance imaging-based stereotactic localization of the globus pallidus and subthalamic nucleus. Neurosurgery 1999;44(2):303–313.
16. Zonenshayn M, Rezai AR, Mogilner AY, Beric A, Sterio D, Kelly PJ. Comparison of anatomic and neurophysiological

methods for subthalamic nucleus targeting. Neurosurgery 2000;47(2):282–292.
17. Patel NK, Heywood P, O'Sullivan K, Love S, Gill SS. MRI-directed subthalamic nucleus surgery for Parkinson's disease. Stereotact Funct Neurosurg 2002;78(3–4):132–145.
18. Slavin KV, Thulborn KR, Wess C, Nersesyan H. Direct visualization of the human subthalamic nucleus with 3T MR imaging. Am J Neuroradiol 2006;27(1):80–84.
19. Cuny E, Guehl D, Burbaud P, Gross C, Dousset V, Rougier A. Lack of agreement between direct magnetic resonance imaging and statistical determination of a subthalamic target: the role of electrophysiological guidance. J Neurosurg 2002;97(3):591–597.
20. Hamani C, Richter EO, Andrade-Souza Y, Hutchison W, Saint-Cyr JA, Lozano AM. Correspondence of microelectrode mapping with magnetic resonance imaging for subthalamic nucleus procedures. Surg Neurol 2005;63(3):249–253.
21. Tasker RR, Organ LW, Hawrylyshyn PA. The thalamus and midbrain of man. In: Wilkins RH, editor. A Physiological Atlas Using Electrical Stimulation. Springfield, IL: Charles C. Thomas; 1982.
22. D'Haese PF, Cetinkaya E, Konrad PE, Kao C, Dawant BM. Computer-aided placement of deep brain stimulators: from planning to intraoperative guidance. IEEE Trans Med Imag 2005;24(11):1469–1478.
23. Nowinski WL, Belov D, Benabid AL. An algorithm for rapid calculation of a probabilistic functional atlas of subcortical structures from electrophysiological data collected during functional neurosurgery procedures. Neuroimage 2003;18(1):143–155.
24. Finnis KW, Starreveld YP, Parrent AG, Sadikot AF, Peters TM. Three-dimensional database of subcortical electrophysiology for image-guided stereotactic functional neurosurgery. IEEE Trans Med Imag 2003;22(1):93–104.
25. Yoshida M. Three-dimensional electrophysiological atlas created by computer mapping of clinical responses elicited on stimulation of human subcortical structures. Stereotact Funct Neurosurg 1993;60(1–3):127–134.
26. Duerden EG, Finnis KW, Peters TM, Sadikot AF. A method for analysis of electrophysiological responses obtained from the motor fibers of the human internal capsule. In: Ellis RE, Peters TM, editors: Proceeding of the Sixth International Conference on Medical Image Computing and Computer-Assisted Intervention (MICCAI 2003), Montreal, Canada, November 2003. Part II. Lecture Notes in Computer Science 2879. Berlin: Springer; 2003. pp 50–57.
27. Starreveld YP. Fast nonlinear registration applied to stereotactic functional neurosurgery. Ph.D. dissertation, University of Western Ontario, London, ON, Canada, June 2002.
28. Holmes CJ, Hoge R, Collins DL, Woods R, Toga AW, Evans AC. Enhancement of MR images using registration for signal averaging. J Comput Assist Tomogr 1998;22(2):324–333.
29. Evans AC, Kamber M, Collins DL, MacDonald D. An MRI based probabilistic atlas of neuroanatomy. In: Shorvon SD, Andermann F, Fish DR, Bydder GM, editors. Magnetic Resonance Scanning and Epilepsy. New York: Plenum Press; 1994. pp 263–274.
30. Guo T, Starreveld YP, Peters TM. Evaluation and validation methods for intersubject non-rigid 3D image registration of the human brain. In: Galloway RL Jr, Cleary KR, editors. Proceeding of SPIE Medical Imaging 2005, San Diego, CA, February 2005. SPIE Vol 5744: Visualization, Image-Guided Procedures and Display. pp 594–603.
31. Herzog J, Fietzek U, Hamel W, Morsnowski A, Steigerwald F, Schrader B, Weinert D, Pfister G, Muller D, Mehdorn HM, Deuschl G, Volkmann J. Most effective stimulation site in subthalamic deep brain stimulation for Parkinson's disease. Movement Disorders 2004;19(9):1050–1054.
32. Laitinen LV, Bergenheim AT, Hariz MI. Leksell's posteroventral pallidotomy in the treatment of Parkinson's disease. J Neurosurg 1992;76(1):53–61.
33. Hubble JP, Busenbark KL, Wilkinson S, Pahwa R, Paulson GW, Lyons K, Koller WC. Effects of thalamic deep brain stimulation based on tremor type and diagnosis. Movement Disorders 1997;12(3):337–341.